

Activation of TRPA1 Channel by Antibacterial Agent Triclosan Induces VEGF Secretion in Human Prostate Cancer Stromal Cells

Sandra Derouiche¹, Pascal Mariot¹, Marine Warnier¹, Eric Vancauwenberghe¹, Gabriel Bidaux¹, Pierre Gosset², Brigitte Mauroy^{1,3}, Jean-Louis Bonnal^{1,3}, Christian Slomianny¹, Philippe Delcourt¹, Etienne Dewailly¹, Natalia Prevarskaya¹, and Morad Roudbaraki¹

Abstract

Accruing evidence indicates that exposure to environmental compounds may adversely affect human health and promote carcinogenesis. Triclosan (TCS), an antimicrobial agent widely used as a preservative in personal care products, has been shown to act as an endocrine disruptor in hormone-dependent tissues. Here, we demonstrate a new molecular mechanism by which TCS stimulates the secretion by human prostate cancer stromal cells of vascular endothelial growth factor (VEGF), a factor known to promote tumor growth. This mechanism involves an increase in intracellular calcium levels due to the direct activation of a membrane ion channel. Using calcium imaging and electrophysiology techniques, we show for the first time that environmentally

relevant concentrations of TCS activate a cation channel of the TRP family, TRPA1 (Transient Receptor Potential Ankyrin 1), in primary cultured human prostate cancer stromal cells. The TCS-induced TRPA1 activation increased basal calcium in stromal cells and stimulated the secretion of VEGF and epithelial cells proliferation. Interestingly, immunofluorescence labeling performed on formalin-fixed paraffin-embedded prostate tissues showed an exclusive expression of the TRPA1 channel in prostate cancer stromal cells. Our data demonstrate an impact of the environmental factor TCS on the tumor microenvironment interactions, by activating a tumor stroma-specific TRPA1 ion channel. *Cancer Prev Res*; 10(3); 177–87. ©2017 AACR.

Introduction

Prostate cancer is among the most frequent malignancies in industrialized nations, and continuous research efforts are undertaken in order to better understand its development and progression. Androgen dependence of this tumors is long known (1–3), but epidemiologic studies suggest that factors from Western life style also contribute to its development (4, 5).

Epithelial stromal interactions are considered important for prostate cancer development and progression (6, 7). Carcinomas in general are composed of two interdependent components: the neoplastic epithelial cells and the supporting tumors stroma, which plays decisive roles in pivotal processes such as tumors proliferation, vascularization, and invasion (8–10) *via*

the secretion of growth factors and cytokines. Following epithelial changes in carcinogenesis, the surrounding stroma is modified by cancer cell-derived factors. These modifications drive the emergence of the characteristic reactive stroma: the modified stromal cells secreting extracellular matrix proteins and soluble factors (cytokines, growth factors), which in turn play important roles in initiation and/or progression of certain carcinomas (11–14), including breast and prostate cancers (9, 15–17). Modulation of these stromal factors secretion might affect the initiation or progression of prostate cancers. In addition to the epithelial-derived and inflammatory factors, environmental molecules might target the stromal cells to modify their physiology, including their secretion capacity. One of the mechanisms involved in the effects of the environmental compounds is the modification of the cellular calcium homeostasis (18). It is well established that Ca^{2+} responses to extracellular stimuli can lead to rapid secretion of growth factors and hormones through exocytosis (19).

Accumulating data indicate that exposure to environmental compounds may adversely affect human health. Triclosan (TCS; 2,4,4'-trichloro-2'-hydroxydiphenyl ether; a chlorophenol) is an antimicrobial agent widely used as preservative in toothpastes, soaps, shampoos, and cosmetics at concentrations up to 0.3% or 10 mmol/L (20). TCS is known to be a highly toxic chemical for aquatic flora and fauna (21) and thus has been included in the probable list of endocrine disruptors (ED). Triclosan is also detected in human blood plasma (22), breast milk (at a concentration of 1–10 μ mol/L; ref. 23), and urine (24), and daily exposure to TCS of breast tissue was estimated to be of

¹Univ. Lille, Inserm, U1003 - PHYCEL - Physiologie Cellulaire, F-59000 Lille, Equipe labellisée par la Ligue Nationale contre le cancer, Villeneuve d'Ascq, France; Laboratory of Excellence, Ion Channels Science and Therapeutics; Université Lille 1 Sciences et Technologies, Villeneuve d'Ascq, France.

²Département de Pathologies, Laboratoire d'Anatomie et de Cytologie Pathologique, Groupe Hospitalier de l'Institut Catholique de Lille (GHICL), Lille, France.

³Service d'Urologie de l'hôpital St-Philibert, Lomme, France.

Note: Supplementary data for this article are available at Cancer Prevention Research Online (<http://cancerprevres.aacrjournals.org/>).

Corresponding Author: Morad Roudbaraki, INSERM U1003, SN3, Université Lille 1 Sciences et Technologies, 59655 Villeneuve d'Ascq, France. Phone: 33-3-20-33-64-23; Fax: 11-33-3-20-43-40-77; E-mail: morad.roudbaraki@univ-lille1.fr

doi: 10.1158/1940-6207.CAPR-16-0257

©2017 American Association for Cancer Research.

Derouiche et al.

5.5 $\mu\text{mol/L}$ (25, 26). At such levels, TCS has been shown to modulate the growth of mammary cancer cells (27), but its potential effects are not known on human prostate cancer epithelial and stromal cells. The mode of action of TCS as an ED is controversial, and it was recently showed that TCS could exert its effects *via* several mechanisms, including the modulation of androgen receptor (28), the modulation of the activity of an adenylyl cyclase enzyme (29) and, recently, the activation of calcium signaling (25). The latter effect of TCS is of importance because it is well established that in most cell types, increase in cell calcium (Ca^{2+}) concentrations is associated with cell growth and/or secretory responses (30).

As epithelial-stromal interactions play a pivotal role in the progression of prostate cancers, environmental factors like TCS may affect these interactions to favor this progression. The present work was designed to determine the effects of TCS on both epithelial and stromal cells derived from prostate cancer tissues. Our work focused on the effects of this environmental factor on calcium signaling, an important parameter controlling the secretion of the mitogenic and/or angiogenic factors by stromal cells known to trigger epithelial and endothelial cells' development.

Using a combination of immunostaining, calcium imaging and electrophysiology techniques, we show here for the first time that the widely used antimicrobial TCS induces the activation of TRPA1 calcium permeable channels and the subsequent release of vascular endothelial growth factor (VEGF) in human prostate cancer stromal cells. We also show the exclusive expression of the TRPA1 protein in stromal cells of human prostate cancer tissue. TCS could thus have a significant impact on prostate carcinogenesis through the activation of TRPA1 channels and subsequent release of VEGF.

Materials and Methods

Chemicals

All chemicals were from Sigma-Aldrich. Triclosan (Irgasan) and triclocarban were dissolved in DMSO, conserved at -20°C and diluted at the desired concentration on the day of the experiments.

Cell lines

LNCaP, PC-3, and DU145 prostate cancer cell lines and the HEK293 (human embryonic kidney-derived 293) cell line were obtained from the American Type Culture Collection (ATCC) and cultured as described by Gackiere and colleagues (31).

Tissue specimens and primary cell cultures

Human prostate cancer biopsies were obtained from consenting patients following the local ethical considerations. All experiments involving patient tissues were carried out under approval number CP 01/33, issued by the Comité Consultatif de Protection des Personnes dans la Recherche Biomédicale de Lille. A portion of prostate tissue suspicious for carcinoma was incised, and one-half of the sliced tissue was submitted for immediate microscopic examination on cryostat sections. After establishment of the diagnosis of adenocarcinoma, the remaining half of the tissue was used for primary culture. The tissue was cut in multiple minute cubicles, placed on a plastic surface, and grown in Phenol red-free RPMI 1640 containing charcoal-stripped fetal calf serum (FCS; CS-RPMI) containing 1 nmol/L DHT for the growth of prostate cancer stromal cells (PrSC) and

in keratinocyte medium supplemented with 50 mg/mL bovine pituitary extract, 5 ng/mL epidermal growth factor (EGF), 100 mg/mL streptomycin, and 100 U/mL penicillin (Life Technologies, Inc.) and 2% FCS for the epithelial cells growth. PrSC cultures were validated by immunofluorescence using anti- α -actin and mouse anti-Vimentin (Dako) antibodies.

Cell transfections and RT-PCR analysis

PrSC were transfected overnight with 25 nmol/L of control siRNA (targeting Luciferase mRNA; Eurogentec) or a siRNA raised against TRPA1 mRNA (siTRPA1-1, target sequence 5'-GGUGG-GAUGUUUUAUCCAUA(dTdT)-3' or siTRPA1-2: 5'-GAAGGACG-CUCUCCACUUA(dTdT)-3') as previously described (32) and used 48-hour posttransfection. The efficiency of the siRNAs was validated by RT-PCR and by Western blot studies (shown for siTRPA1-1 in Fig. 2D). RT-PCR experiments and HEK293 stably transfected by either hTRPA1 coding sequence (HEK-hTRPA1) or by pcDNA3 vector (HEK-vector) were realized as described earlier (32). The PCR primers (hTRPA1: 5'-AGTGGCAATGTGGAGCAA-3' and 5'-TCTGATCCACTTTGCGTA-3'; β -actin: 5'-CAGAGCAA-GAGAGGCATCCT-3' and 5'-GTTGAAGTCTCAAACATGATC-3' used in this study were designed on the basis of established GenBank sequences and synthesized by Invitrogen. The amplified PCR products were of 510 and 212 bp, respectively.

Immunofluorescence studies

The protein expression studies of the ion channels in prostate cancer cells and tissues were determined by indirect immunofluorescence analysis performed on acetone-fixed cells and formalin-fixed paraffin embedded (FFPE) tissues as previously described (32) and analyzed by confocal microscopy (Zeiss LSM 780; acquisition parameters: objective $40\times/1.3$; thickness of confocal slide, 1 μm). Three prostate non-cancer and four prostate cancer tissues were used in the present work to study the expression of the TRPA1 channel. The prostate cancer tissues were from 54-, 60-, 61-, 76-year-old patients all presenting the same TNM (T2N0M0) with Gleason grades of 3, 3, 4, and 4 and Gleason scores of 6, 5, 7, and 7, respectively. For the expression of the TRPA1 channel in breast cancer, two grade 2 breast carcinoma (infiltrating ductal carcinoma) from 52- and 61-year-old patients were used, and the expression of the channel was examined in cancer and in the adjacent non-cancer regions.

Western blot assay

PrSC and HEK293 cells were cultured at 80% of confluence and total proteins extracted. Ten to μm of each sample were analyzed by Western blotting using hTRPA1 (Alomone Labs, 1/500e) β -actin (Sigma-Aldrich, 1/2000e) and Calnexin (Santa Cruz Biotechnology, 1/200e) antibodies and ECL technique as described previously (32).

Cytosolic free Ca^{2+} concentration ($[\text{Ca}^{2+}]_i$) measurements

Cells were grown on glass coverslips, and $[\text{Ca}^{2+}]_i$ imaging experiments were performed in Hanks Balanced Salt Solution (HBSS) in mmol/L: 142 NaCl, 5.6 KCl, 1 MgCl_2 , 2 M CaCl_2 , 0.34 Na_2PO_4 , 0.44 KH_2PO_4 , 10 HEPES, 5.6 glucose, and buffered to pH 7.4, as previously described (32) using Fura-2 AM as calcium dye. To represent the variation of the $[\text{Ca}^{2+}]_i$, the fluorescence intensity ratio represented by F340/F380 was used as an indicator of changes in cytosolic Ca^{2+} concentration. Each experiment was repeated at least 4 times in duplicate on different cell cultures

on a field of 35 to 45 cells and representative experiments performed on 60 to 90 cells as mean \pm SE are presented.

Electrophysiological studies

Whole-cell patch-clamp recordings were performed using a RK-300 patch-clamp amplifier (Biologic) as previously described (31). Bath medium used for whole-cell experiments consisted in HBSS supplemented with 10 mmol/L TEA to block potassium currents. Recording pipettes were filled with a solution containing (in mmol/L) 140 Kgluconate, 10 NaCl, 10 HEPES, 2 MgCl₂, with 1 EGTA. Osmolarity and pH were adjusted to 290 mOsm.L⁻¹ and 7.2, respectively.

Preparation of PrSC-conditioned medium and cell growth studies

Primary cultured stromal cells (5×10^5 cells per condition) were cultured in CS-RPMI supplemented with 0.1% FCS with or without TCS for 3 days. Culture supernatants were collected, centrifuged, and then incubated with PC-3 cells for the cell growth studies. PC-3 cells seeded in 96-well plates (3,000 cells/well) were cultured in RPMI/10% FCS for 24 hours. The medium was then replaced by 150 μ L of PrSC-conditioned medium and incubated for 3 days. The control PC3 cells were cultured in CS-RPMI supplemented with 0.1% FCS for 3 days with or without TCS. Cell growth was estimated using the commercial assay MTS/PMS kit as previously described (32). PC-3 cell proliferation assays were also evaluated by Malassez manual cell counting. Briefly, PC-3 cells were cultured in 12-well plates (4-well per condition) and after incubation periods, cells were trypsinized and suspended in 500 μ L PBS and 10 μ L of each sample were used for manual cell counting. Each sample was counted at least twice, and the results are expressed in number of cells. Assays were performed in triplicate. Differences between samples and the corresponding control (CTL) were determined by the one-way ANOVA analysis, where $P < 0.05$ was considered statistically significant.

ELISA for VEGF

PrSC cells were incubated in CS-RPMI supplemented with 0.1% FCS with or without TCS for 3 days into 12-well plates. The supernatants of the cell cultures were then withdrawn, centrifuged, and a VEGF immunoassay kit (Abcam) was used for VEGF detection according to the manufacturer's instructions.

Statistical analysis

Plots were produced using Origin 8.0 (Microcal Software). Results are expressed as mean \pm SE. Statistical analysis was performed using unpaired t tests or ANOVA tests followed by either Dunnett (for multiple control vs. test comparisons) or Student–Newman–Keuls posttests (for multiple comparisons). The Student t test was used for statistical comparison of the differences, and $P < 0.05$ was considered statistically significant.

Results

Triclosan induces calcium signaling in human PrSC

We first assessed the effects of Triclosan (TCS) and its structural analog, Triclocarban (TCC) on prostate cancer stromal cells. The PrSC primary culture were first characterized for

the expression of stromal cells markers by immunofluorescence studies using antibodies raised against α -actin and vimentin. Seven different cultures originated from 7 patients were included in this study. We observed that the proportion of cells expressing α -actin and/or vimentin varied between each primary cell culture. Globally, the PrSC cultures were divided in two categories, the first one in which 90% of cells expressed vimentin (fibroblasts) and the remaining 10% expressed α -actin (smooth muscle cells; Fig. 1C, inset), and the other one in which almost 100% of cells expressed both vimentin and α -actin (myofibroblasts; Fig. 1D, inset), suggesting the presence of only stromal cells in our cultures.

On these characterized stromal cells, by calcium imaging, we studied the effects of TCS and its structural analogue, TCC (see chemical structures in insets in Fig. 1A and B), on cytosolic free calcium concentration ($[Ca^{2+}]_i$). The $[Ca^{2+}]_i$ was continuously monitored as a fluorescence ratio F340/F380 using the calcium probe Fura-2/AM in a normal HBSS medium containing 2 mmol/L CaCl₂ and then, at the time indicated, TCS or TCC was applied to the cells. In these experiments, TCS induced a rapid and dose-dependent increase in $[Ca^{2+}]_i$ in PrSC (Fig. 1A). These observations suggest that TCS is able to induce either a calcium entry and/or a Ca²⁺ release from intracellular stores. In the same experimental conditions, TCC failed to elicit any significant modulation of basal $[Ca^{2+}]_i$ in PrSC (Fig. 1B). Two types of TCS-induced calcium increase were observed with regard to the kinetics and amplitudes (Fig. 1C and D). TCS induced an initial rapid and transient first phase followed by a sustained plateau phase characterized by either a low (Fig. 1C) or a high amplitude (Fig. 1D). The combined calcium imaging and immunofluorescence studies using α -actin and vimentin antibodies suggest that these two different types of calcium response are correlated with the preponderance of myofibroblasts for the high-amplitude plateau phase (Fig. 1D) and with the preponderance of fibroblasts for the low-amplitude plateau phase (Fig. 1C) in stromal cells populations. This robust effect of TCS on calcium entry was observed on PrSC from 6 out of 7 cancer tissues.

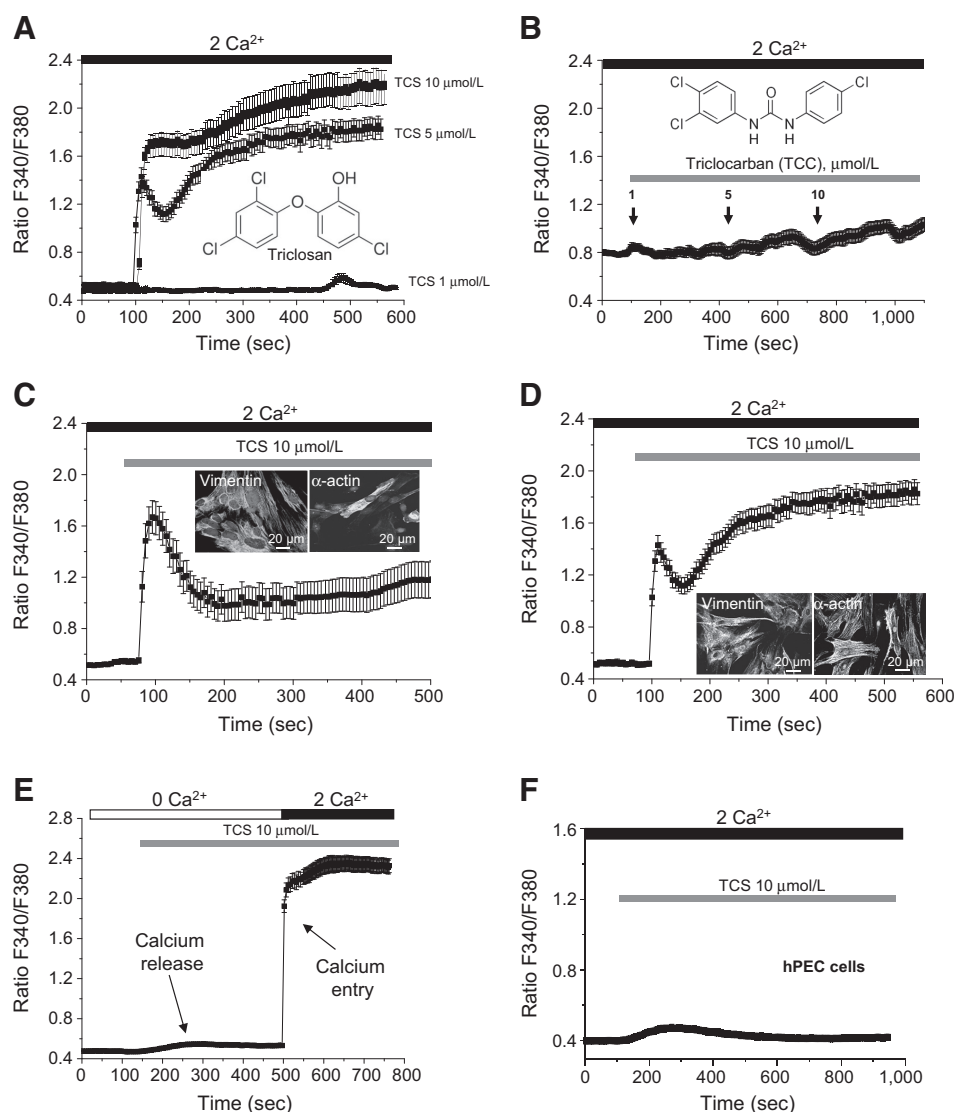
The origin of the TCS-induced calcium increase in human prostate stromal cells

In calcium imaging experiments, cells were challenged with TCS in a Ca²⁺-free HBSS medium (Fig. 1E) followed by the addition of 2 mmol/L calcium still in the presence of TCS. In the absence of external calcium, TCS induced a slight calcium response due to a mobilization of calcium from intracellular pools, through the activation of Type I Ryanodine Receptors (RyRs) as previously described in mouse skeletal myotubes (25). Interestingly, as shown in Fig. 1E, when calcium was added in the external buffer, TCS induced a rapid and high-amplitude calcium entry in human PrSC via the plasma membrane calcium channels. The same experiments performed on human prostate cancer epithelial cells (hPEC) showed that TCS only induced a calcium mobilization without promoting a calcium entry in these cells (Fig. 1F). We therefore undertook experiments in order to identify the calcium permeable membrane channels involved in the effects of TCS in primary cultured PrSC.

Involvement of TRPA1 in TCS-induced calcium response

To investigate the membrane ion channels involved in TCS-induced calcium entry, we used an extensive

Derouiche et al.

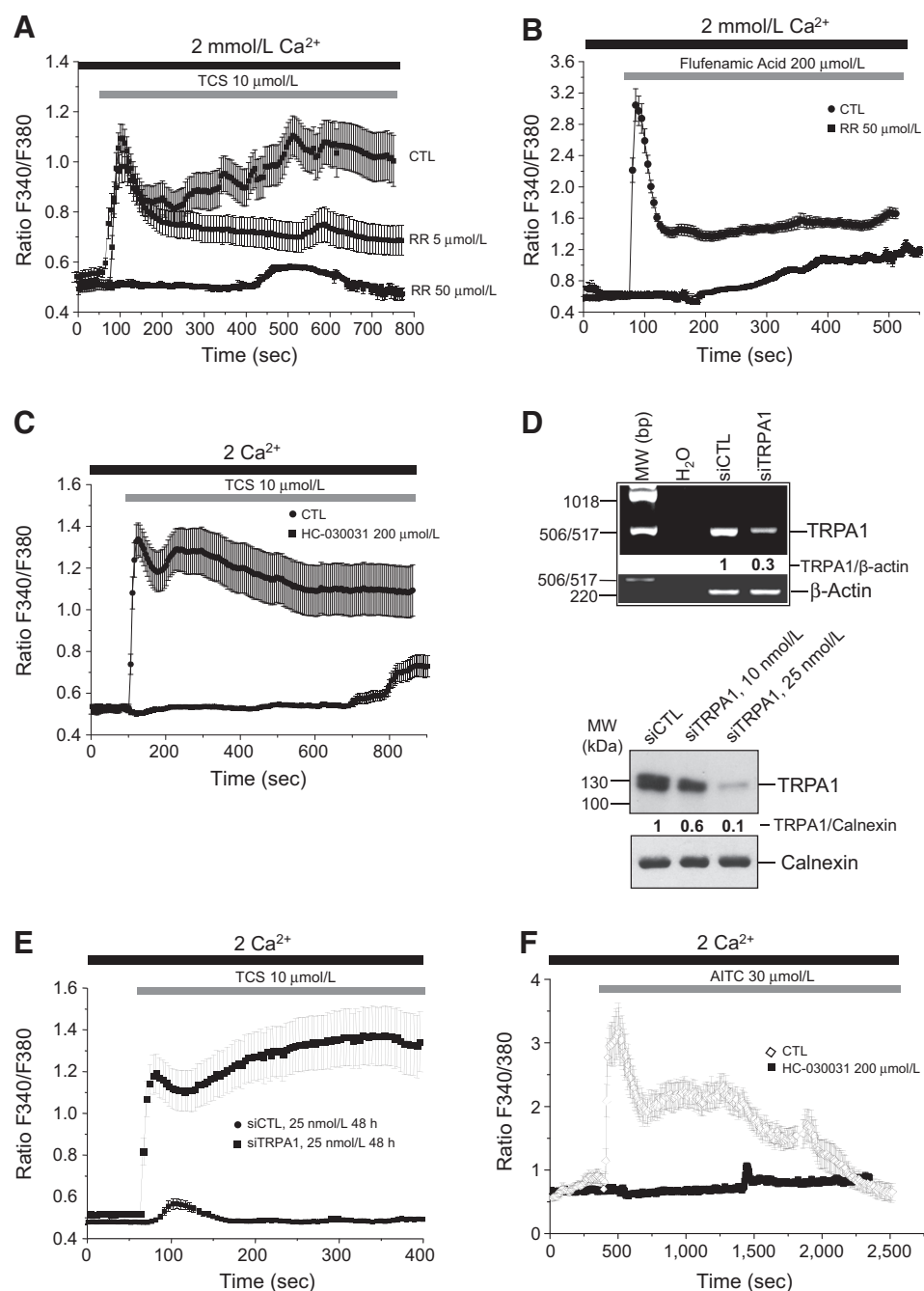
**Figure 1.**

Effects of TCS and TCC on basal $[Ca^{2+}]_i$ of stromal cells derived from prostate cancer. Direct effects of TCS (**A**) or its analogue TCC (**B**) at different concentrations on $[Ca^{2+}]_i$ were studied by calcium imaging in a 2 mmol/L $CaCl_2$ medium (2 Ca^{2+}). Insets show the respective chemical structure of each compound. TCS induced two types of calcium response depending on the composition of stromal cell population: transient with a subsequent low amplitude plateau phase (**C**) and transient with a subsequent high-amplitude plateau phase (**D**). Insets in **C** and **D** present the expression of the α -actin and vimentin in two different primary cultures of PrSC. To determine the origin of the TCS-induced calcium response, cells were first placed in a Ca^{2+} -free bath solution (0 Ca^{2+}) and then exposed to 2 mmol/L extracellular Ca^{2+} (2 Ca^{2+}) as indicated (**E**). Effect of TCS on $[Ca^{2+}]_i$ in human primary epithelial cells (hPEC; **F**). The TCS application and presence or absence of extracellular Ca^{2+} are marked by horizontal bars. Each experiment was repeated at least 5 times in triplicate on different cell cultures on a field of 25 to 40 cells, and representative figures are presented for each experiment.

pharmacology comprising blockers of voltage-dependent, non-voltage-dependent calcium channels and potassium channels (Supplementary Fig. S1A). Surprisingly, many tested blockers [inhibitors of L-Type voltage-dependent calcium channels and non-voltage-dependent calcium channels (TRP)] were able to elicit an increase in $[Ca^{2+}]_i$ somehow similar to the one induced by TCS (Supplementary Fig. S1B and S1C). According to the published data, all these compounds were activators of a unique ion channel, the non-voltage-dependent TRPA1 calcium channel (33–37). We thus assessed whether TRPA1 could be the ion channel activated by TCS in human PrSC.

We first used ruthenium red (RR) as a non-selective inhibitor of TRPA1 channel. As shown in Fig. 2A, the TCS-induced calcium entry was dose dependently blocked by RR. Moreover, the calcium increase observed by application of flufenamic acid was also inhibited by ruthenium red (Fig. 2B), suggesting the involvement of TRPA1 in flufenamic acid effects in these cells. We next used a selective inhibitor of TRPA1 channel, the compound HC-030031, which showed a dose-dependent inhib-

itory effect on the TCS-induced calcium response with a maximal inhibition for a concentration of 200 μ mol/L (Fig. 2C and Supplementary Fig. S2A–S2F). The involvement of the TRPA1 channel in the TCS-induced calcium response was confirmed by the use of AP-18 and A967079, two other inhibitors of the TRPA1 channel (Supplementary Fig. S3A–S2F). In these experiments, we also observed a significant decrease in basal calcium concentration after the addition of HC-030031 (200 μ mol/L) and RR (50 μ mol/L; Fig. 2B and C). These observations suggest that TRPA1 is involved in setting the basal calcium concentration in PrSC. To confirm these results, we also used siRNAs targeting TRPA1 (siTRPA1) to downregulate the TRPA1 protein. Using RT-PCR and Western blot techniques, we first showed that the siTRPA1 transfection (25 nmol/L) of stromal cells induced a significant downregulation of the TRPA1 mRNA and protein in these cells (Fig. 2D). We then observed in calcium experiments that the TCS-induced calcium entry was almost completely blocked in siTRPA1-transfected cells (Fig. 2E), leading to the conclusion that TRPA1 is the main ion channel involved in TCS-induced calcium entry. To confirm the functionality of TRPA1

**Figure 2.**

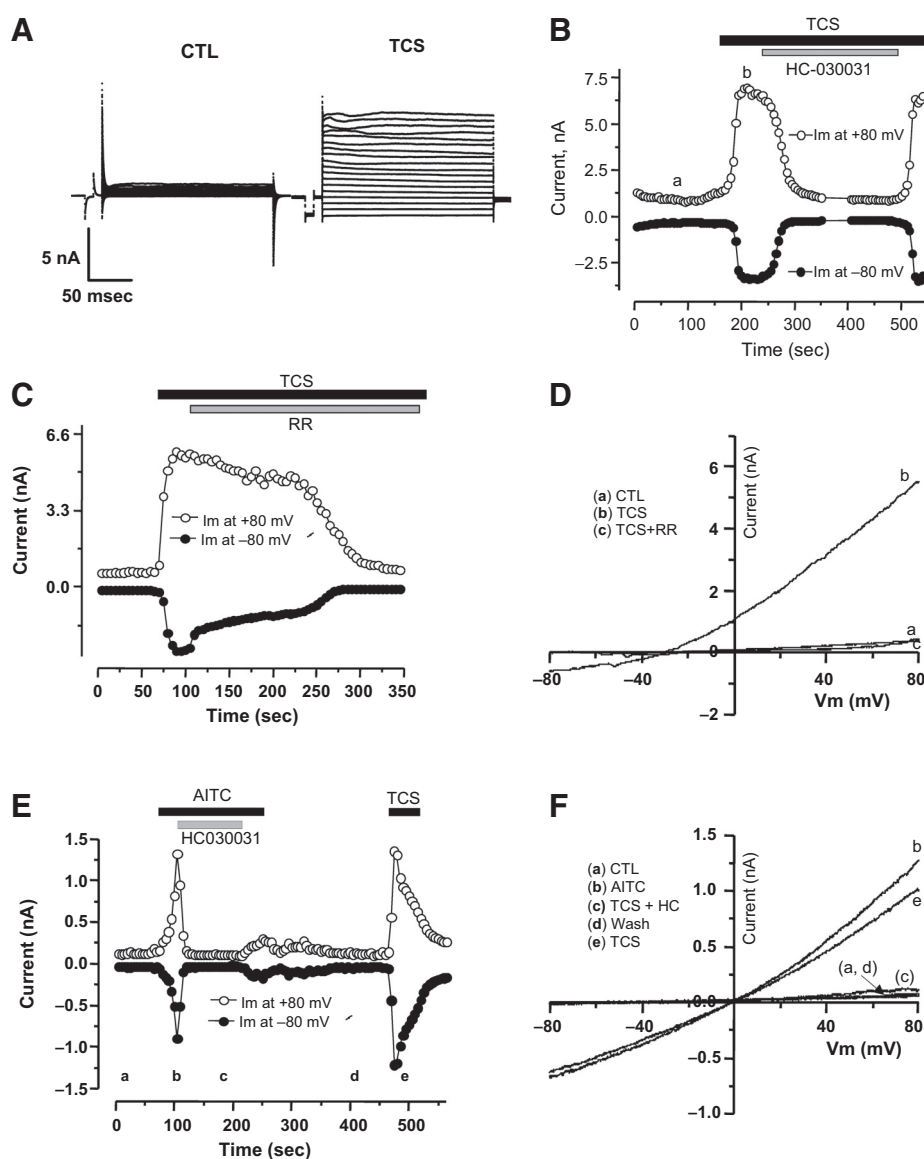
Suppression of TCS-induced calcium entry by inhibition of TRPA1 in PrSC. Calcium imaging experiment in the presence of TCS (**A**) or flufenamic acid (**B**) combined with the nonspecific TRPA1 inhibitor, Ruthenium Red (RR). **C**, TCS-induced calcium increase in the presence of the specific inhibitor HC-030031. **D**, RT-PCR and Western blot performed on PrSC transfected with control siRNA (siCTL) or siTRPA1-1 (25 nmol/L). The corresponding calcium imaging experiments in siCTL- and siTRPA1-transfected cells is shown in **E**. The functionality of TRPA1 was studied by the application of a known TRPA1 agonist (AITC) in the absence or presence of the TRPA1 inhibitor (HC-030031, 200 μmol/L; **F**). Each experiment was repeated at least 3 times in triplicate on different cell cultures on a field of 25 to 40 cells, and representative figures are presented for each experiment.

channel in prostate cancer stromal cells, the effects of a known TRPA1 agonist (Allyl Isothiocyanate, AITC) on cytosolic free calcium concentration were studied in PrSC. As shown in Fig. 2F, AITC (30 μmol/L) induced a calcium increase which was inhibited by HC-030031 (200 μmol/L).

We further investigated the potential activation of TRPA1 by TCS in PrSC by electrophysiological approaches using whole-cell patch clamp techniques. A voltage ramp of -80 to +80 mV was applied, and the resulting currents were recorded in the absence (CTL) or in the presence of TCS in the extracellular medium. As shown in Fig. 3A-D, TCS induced within few seconds after the onset of perfusion a large increase in mem-

brane conductance at all membrane potentials. TCS-induced membrane current displayed a slight outward rectification and reversed around 0 mV. This TCS-induced current was reversible when cells were washed with TCS-free HBSS and was inhibited by the addition of HC-030031 (50 μmol/L). The action of TCS was similar to that of AITC, which was able to activate TRPA1 current in PrSC, an effect also inhibited by HC-030031 (50 μmol/L; Fig. 3E and F). To confirm the implication of TRPA1 in TCS-induced current, the effects of TCS were studied in HEK-hTRPA1 cells stably expressing the human form of TRPA1. In these cells, both TCS (10 μmol/L) and AITC (50 μmol/L) reversibly increased membrane conductance, as

Derouiche et al.

**Figure 3.**

Electrophysiological studies of the TCS-induced TRPA1 activation in PrSC. TCS (10 $\mu\text{mol/L}$) increased whole-cell currents at all membrane potentials ranging from -100 to 120 mV in PrSC (**A**). **B**, Representative time courses of whole-cell currents in PrSC measured at membrane potentials of -150 mV (red circles) and $+150$ mV (black circles) with punctual administrations of HC-030031 (50 $\mu\text{mol/L}$). **C** and **D**, Representative time courses and current-voltage (I-V) relationships of whole-cell currents in PrSC showing that TCS (10 $\mu\text{mol/L}$)-induced currents (b) was suppressed by Ruthenium Red (RR, 50 $\mu\text{mol/L}$; c). **E** and **F**, Representative time courses (a) and current-voltage (I-V) relationships (b) of whole-cell currents in PrSC showing that TCS (10 $\mu\text{mol/L}$)-induced currents were similar to AITC (30 $\mu\text{mol/L}$)-induced currents which were also inhibited by HC-030031 (HC, 50 $\mu\text{mol/L}$).

in stromal cells, whereas they were ineffective in vector-transfected cells (HEK-vector cells; Fig. 4A–D). Moreover, TCS- and AITC-induced currents were also inhibited by HC-030031 (50 $\mu\text{mol/L}$). These data clearly show that the antibacterial TCS induces the activation of hTRPA1.

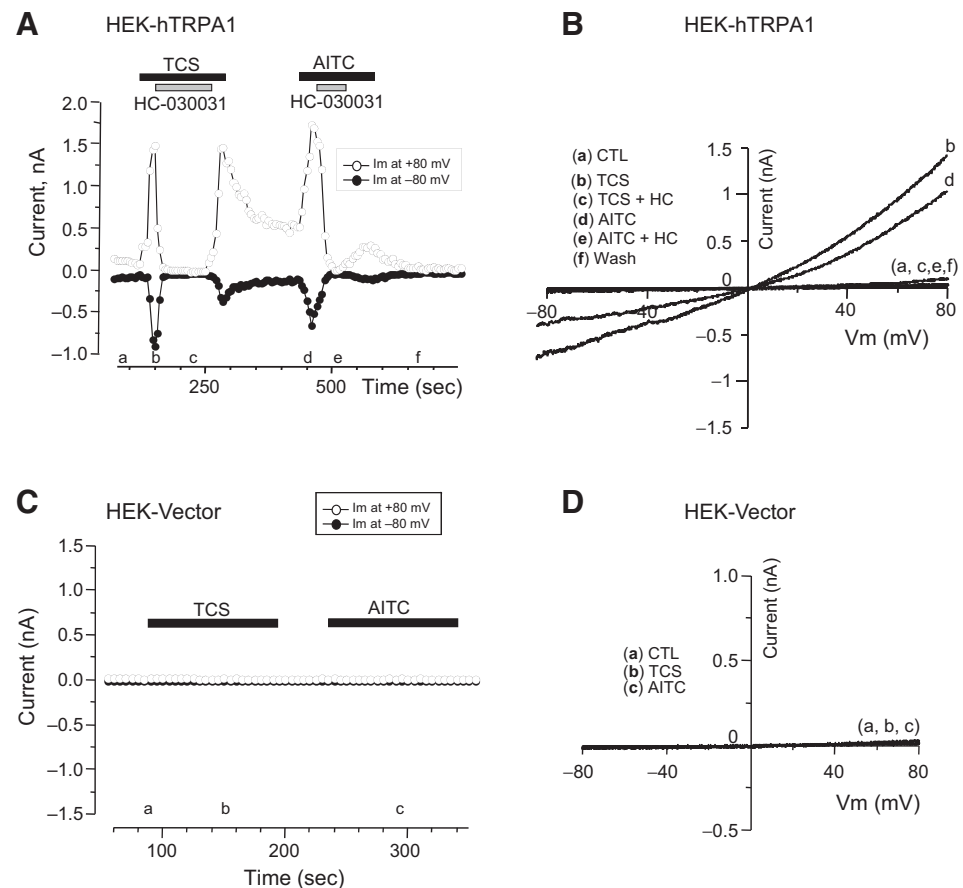
Expression of TRPA1 channel in the human prostate cancer

We further studied the expression of the TRPA1 channel in PrSC and human prostate cancer epithelial cells. First, by RT-PCR analysis, we observed an absence of TRPA1 expression in epithelial cells while stromal cells obtained from different prostate cancer tissues all expressed the mRNA for TRPA1 (Fig. 5A). TRPA1 expression was also confirmed in HEK-hTRPA1 cells by Western blot experiments. As shown in Fig. 5B, the antibody revealed a band of expected size (~ 130 kDa) and a band of higher molecular weight, which could represent a glycosylated form of TRPA1 protein. The same antibody was then used in Western blot experiments performed on different prostate cancer epithelial cell lines (LNCaP and PC-3), primary cultured epithelial cells

(hPEC) and stromal cells of different patients (PrSC) used in the present study. As shown in Fig. 5C, the TRPA1 proteins were present only in protein extracts from stromal cells. This is in agreement with our results showing a stimulation of an HC-030031-sensitive calcium entry by TCS in stromal but not in epithelial cells. We further studied by immunofluorescence staining the expression of the TRPA1 channel protein in 7 different non-cancer (BPH) and cancer (prostate cancer) tissues using formalin-fixed, paraffin-embedded tissues. As α -actin (smooth muscle actin) expression was restricted to the stroma, the positive staining for α -actin was used to discriminate between the epithelium and the stroma. Coimmunolabeling for TRPA1 (in green) and α -actin (in red) showed overlapping staining in prostate cancer regions showing a preferential expression of TRPA1 protein in stromal cells of the cancer regions (Fig. 5D and E) and in the primary culture stromal cells (Fig. 5F). The same coimmunolabeling experiments performed in non-cancer (BPH) regions did not reveal any staining for the TRPA1 protein neither in epithelial cells nor in stromal cells (Fig. 5H), whereas α -actin (in red) was

Figure 4.

TCS-induced ion currents in HEK-hTRPA1 cells. Electrophysiological studies were carried out in HEK293 cells transfected either with vector alone (HEK-vector) or with human TRPA1 coding sequences (HEK-hTRPA1). Representative time courses measured at a membrane potential of -80 mV (red circles) and ± 80 mV (A) and current-voltage (I-V) relationships (B) of whole-cell currents recorded in HEK-hTRPA1 cells. The application of TCS (10 $\mu\text{mol/L}$) induced similar currents to that of induced by AITC (30 $\mu\text{mol/L}$). Both AITC and TCS-induced currents were inhibited by HC-030031 (HC, 50 $\mu\text{mol/L}$). Representative time courses measured at a membrane potential of -80 mV (red circles) and ± 80 mV (C) and current-voltage (I-V) relationships (D) of whole-cell currents recorded in HEK-vector cells. The drug applications are marked by horizontal bars.



clearly expressed in stromal cells (Fig. 5G and H). A control immunofluorescence experiment is presented (Fig. 5I), where the primary antibody (anti-TRPA1) was omitted.

These data clearly show the preferential expression of TRPA1 in prostate cancer stromal cells. To extend these data to other cancers, we studied the expression of TRPA1 in 3 breast non-cancer and cancer tissues. As shown in Fig. 5J-L, TRPA1 protein is increased in cancer regions of breast tissues. These data suggest a common feature of TRPA1 expression in cancer and that the effects of TCS on TRPA1 channels could be of importance in cancer progression by inducing calcium entry and a possible secretion of factors necessary for the epithelium-stroma interactions.

Triclosan induces VEGF secretion by stromal cells

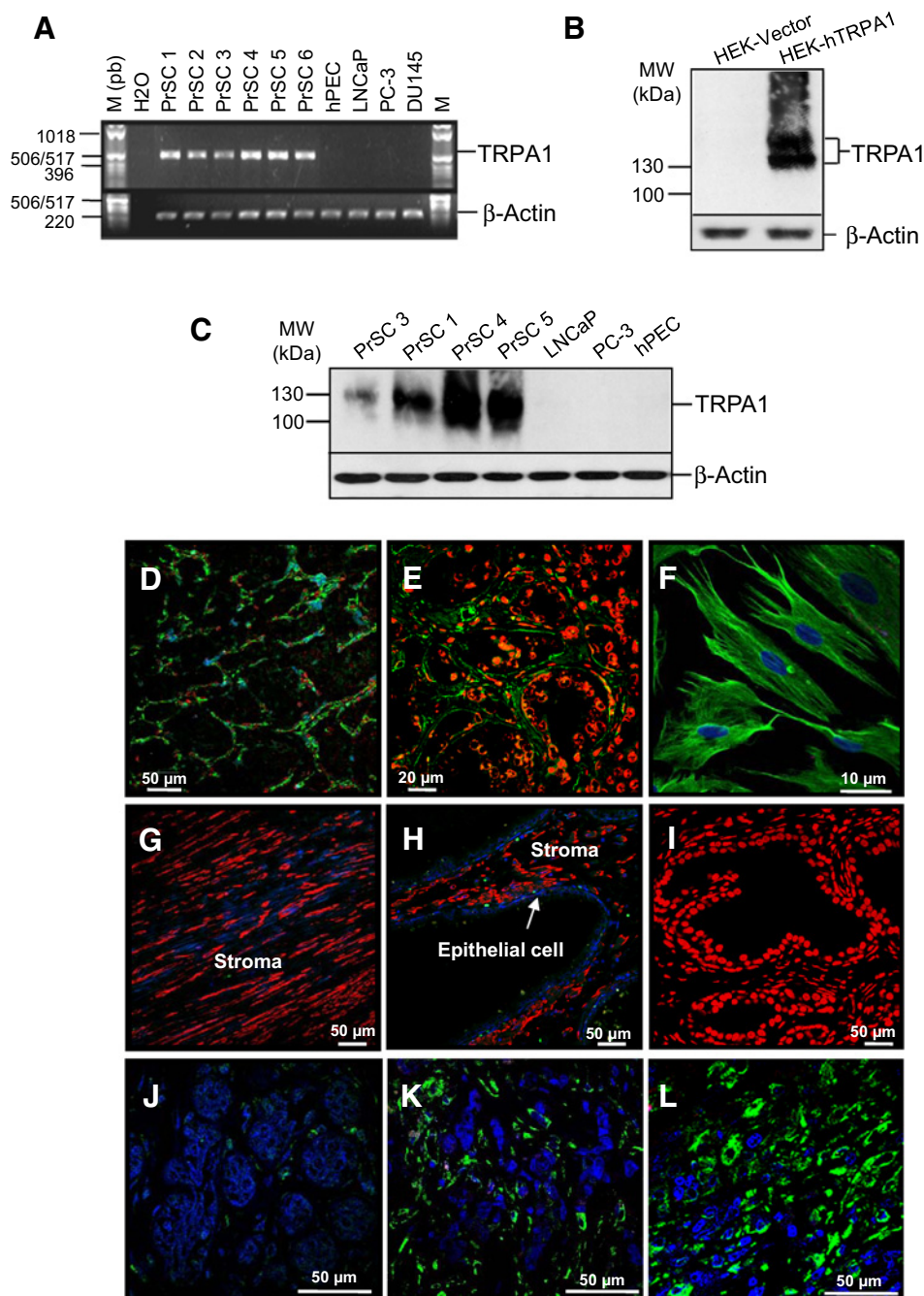
To assess the influence of TCS on epithelial-stromal interactions, we examined the impact of TCS pretreatments of PrSC on the proliferation of PC-3 prostate cancer epithelial cells. In this context, using the MTS assay, we observed that when PrSC cells were cultured in CS-RPMI supplemented with 10% FCS, the PrSC-conditioned media stimulated an increase in proliferation of PC-3 cells. When PrSCs were cultured in CS-RPMI with 0.1% FCS, the PrSC-conditioned media failed to stimulate the proliferation of PC-3 cells. Interestingly, in this low serum condition, the conditioned media from TCS-pretreated PrSC induced an increase in PC-3 cells growth (Fig. 6A), whereas in high serum condition (10% FCS), the conditioned media of TCS-treated PrSC induced only a faint increase of the PC-3 cell proliferation (data not shown). These observations were con-

firmed when the experiments were performed by manual cell counting technique (Fig. 6B). We then carried out ELISA measurements of growth factors secretion in CTL and TCS-treated-conditioned media of PrSC. Interestingly, the incubation of stromal cells with TCS (1 – 10 $\mu\text{mol/L}$) clearly induced an increase in VEGF secretion (Fig. 6C). In addition, TCS-induced VEGF secretion was inhibited by the TRPA1 inhibitor HC-030031, suggesting the involvement of the TRPA1 channel in the effects of TCS on VEGF secretion by prostate stromal cells. In these experiments, the TRPA1 inhibitor HC-030031 showed a dose-dependent inhibitory effect on the TCS-induced VEGF secretion reaching a maximum of inhibition for a concentration of 200 $\mu\text{mol/L}$ (Fig. 6C and Supplementary Fig. S4). The involvement of TRPA1 channel in the TCS-induced VEGF secretion was confirmed by the use of AP-18 and A967079, two other inhibitors of TRPA1 channel (Supplementary Fig. S4). These data suggest that TCS, by stimulating the secretion of factors by stromal cells, might promote prostate tumorigenesis (Fig. 6D).

Discussion

The present study reports for the first time the potential impact of TCS, a widely used antibacterial in cosmetics and hygienic products, on human prostate cancer-associated stromal cells. Indeed, we have shown that TCS induced an important calcium entry in primary cultured stromal cells of human prostate cancer tissues by activating the TRPA1 channel.

Derouiche et al.

**Figure 5.**

TRPA1 channel expression prostate cancer tissues. The TRPA1 channel expression was assessed by RT-PCR (**A**) and Western blotting (**B** and **C**) in stromal cells derived from human prostate cancer (PrSC, numbers indicate PrSC from different patients), prostate epithelial cells (LNCaP, PC-3, and DU145 prostate cancer cell lines and hPEC primary epithelial cells), HEK-vector and HEK-hTRPA1 cells. Semiquantitative RT-PCR experiments were performed to study the expression of TRPA1 (510 bp) mRNA using specific primers. To detect TRPA1 protein, 20 μ g total proteins were analyzed by Western blot using a TRPA1-specific antibody. Immunofluorescence studies using a TRPA1 antibody (green) were performed on grade 3 prostate cancer FFPE tissues (**D** and **E**), on primary stromal cells PrSC (**F**) and on normal prostate and BPH FFPE tissues (**G** and **H**). Nuclei were either stained by DAPI (blue) or propidium iodide (red). The panel (**I**) shows the control experiment where the primary antibody was omitted and only the nuclei were stained by propidium iodide (PI). Immunofluorescence studies performed on normal breast (**J**) and breast cancer tissues (**K** and **L**) using the TRPA1 antibody (green) and DAPI staining for the nuclei (blue).

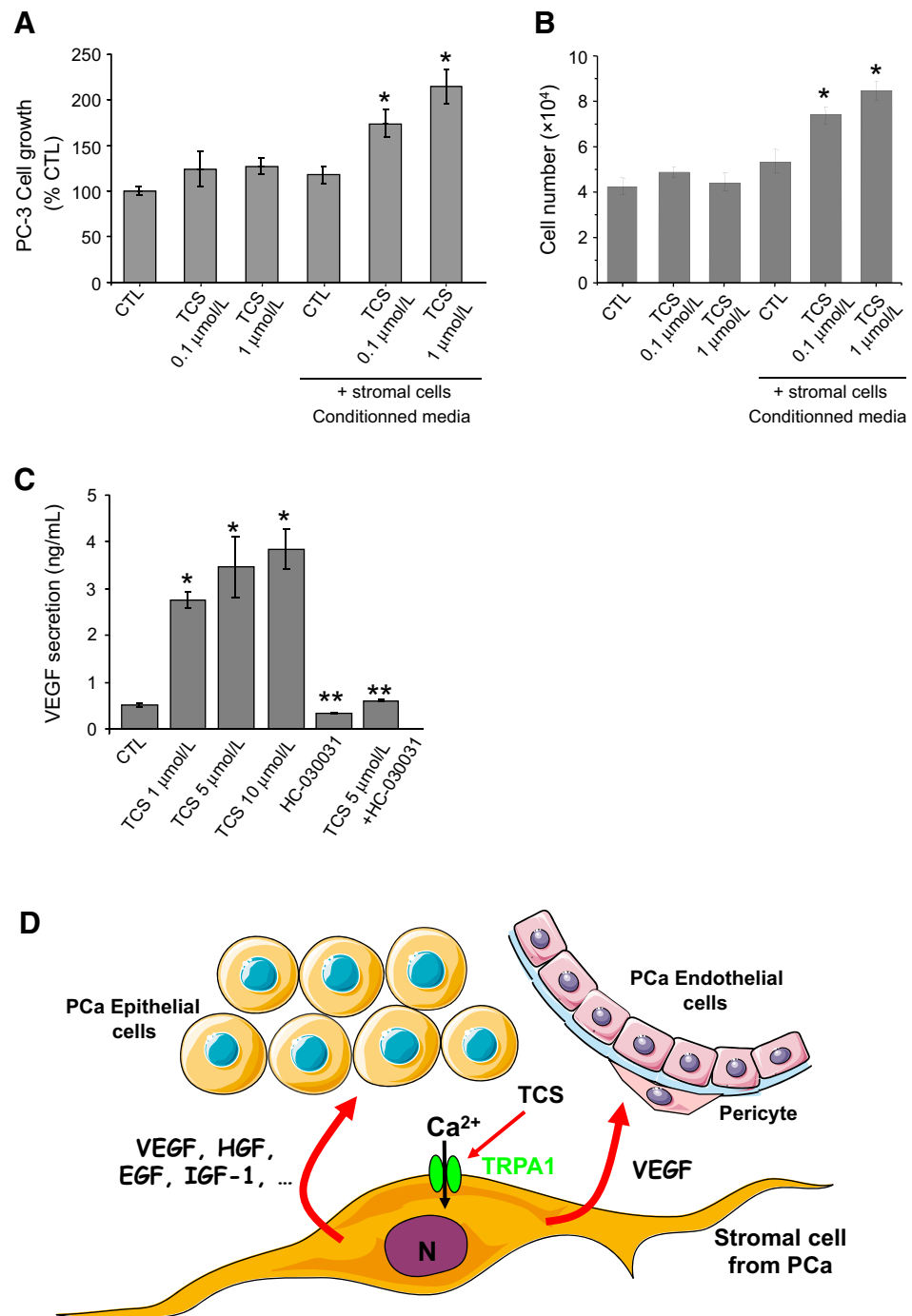
The TRPA1 channel has been studied for its role in the (patho)physiology of several organs and its potential as a drug target for the management of various pathologic conditions has previously been suggested (38, 39). Initially reported to detect noxious cold (40), TRPA1 receptors have subsequently been shown to act as sensors of many environmental irritants, including acrolein, formaldehyde, zinc, pungent plant ingredients such as mustard oil, cinnamaldehyde, and allicin, as well as endogenously produced substances such as hydrogen peroxide and 4-hydroxynonenal (38). Our data suggest that the antimicrobial agent TCS has to be included in the long list of

environmental factors inducing TRPA1 channel activation. However, the fixation site of TCS on the TRPA1 channel needs further investigations, using channel mutants in different intracellular and extracellular ligand binding domains of the channel.

We have also shown here for the first time the exclusive expression of TRPA1 channels in human PrSC. According to the published data, the stroma is transformed into "reactive stroma" during early prostate cancer development and it co-evolves with the cancer progression. Previous studies have established that reactive stroma biology influences prostate tumorigenesis

Figure 6.

TCS induces mitogenic factor secretion. **A**, 3×10^3 PC-3 cells grown in 96 well plate in complete medium were either treated with 0.1% FCS medium containing or not TCS (0.1 or $1 \mu\text{mol/L}$) or with media conditioned by PrSC cells exposed or not to TCS (0.1 or $1 \mu\text{mol/L}$) for 3 days. MTS assay was then performed and mean data of viable cells are represented. *, $P < 0.001$ relative to CTL conditions. **B**, PC-3 cell proliferation assays were also evaluated by Malassez manual cell counting as described in *materials and methods*. Assays were performed in triplicate. Differences between samples and the corresponding control (CTL) were determined by the one-way ANOVA analysis, where $P < 0.05$ was considered significant. **C**, Quantitative measurement of human VEGF by ELISA in the conditioned media of PrSC cells. Stromal prostate cancer cells were cultured for 4 days in presence or not of TCS (1, 5 or $10 \mu\text{mol/L}$) and HC-030031 (200 $\mu\text{mol/L}$). Experiments were performed as described in *materials and methods* and results are shown as the mean \pm SE. Experiments were repeated four times in independent primary cell cultures and a representative figure is presented. Results are presented as the percentage of control (CTL). *, $P < 0.01$ relative to CTL condition; **, $P < 0.001$ TCS $5 \mu\text{mol/L}$ versus TCS $5 \mu\text{mol/L}$ + HC-030031 200 $\mu\text{mol/L}$. **D**, Hypothetic TCS-activated pathways in PrSC: TCS, by modifying calcium signaling through TRPA1, could trigger stromal cells secretion of mitogenic factors, leading to the proliferation and/or the migration of prostate cancer epithelial and vascular endothelial cells (angiogenesis), two important components of tumor formation.



and progression. In the present work, we show that TCS, via activation of TRPA1, induces VEGF secretion. The VEGF receptors have been shown to be present in epithelial, stromal, and endothelial cells (41), suggesting a complex interplay between the cell components of the prostate cancer microenvironment. VEGF can potentiate different functions in prostate cancer, many of which may be responsible for its growth and survival in the androgen-refractory stage, the aggressive form of the disease. The main function of VEGF is its involvement

in lymphangiogenesis where the growth and sprouting of lymphatic endothelium occurs from a preexisting lymphatic vessel (42). Increased lymphatic vessel formation surrounding a tumor may provide potential routes for tumor cells to migrate to distant organs. As a first line of treatment, androgen-deprivation therapy triggers tumor growth arrest and tumor apoptosis in the primary site, and therefore an increase in the metastatic potential that helps the tumor cells to migrate to a different location and survive. Interestingly, several works have

Derouiche et al.

shown the potential VEGF-mediated function that may be important for the growth and survival of prostate cancer from its early phases to transition to the androgen-refractory stage (41). Thus, TCS-induced VEGF secretion might favor the progression of prostate cancer by modulating the growth and transformation of prostate epithelial cells, angiogenesis, and finally metastasis. These aspects need to be investigated in *in vivo* studies to address the impact of TCS on the prostate cancer epithelial–stromal and stromal–endothelial cell interactions. Secondly, the impact of TCS on the cancer cell tumor development (in nude mice) and the potential variations of vessel density in these prostate cancer cell xenografts require further investigations. In this context, our preliminary work showed that the TCS and AITC treatment of nude mice coinjected with human prostate cancer epithelial and stromal cells promoted tumor development. These data suggest that targeting the TRPA1 channel could be an alternative to the actual therapies (AR ablation) leading to relapse in the majority of cases.

In addition to environmental factors, several endogenous TRPA1 activators have also been detected. These may modulate the secretion of paracrine factors by stromal cells. TRPA1 is an attractive candidate, because it can be activated by molecules that are produced during oxidative phosphorylation, such as hydrogen peroxide (H₂O₂), 4-Hydroxynonenal (4-HNE), cyclopentenone prostaglandins (PGJ₂; ref. 43), and Methylglyoxal, formed from triose phosphates during secondary glucose metabolism in hyperglycemic condition (39). Recently, TRPA1 has also been shown to be activated by formaldehyde (44).

Interestingly, clinical data have shown that formaldehyde concentration is elevated (2.8-fold) in the urine of patients with prostate and bladder cancer (45) and in the expired air from tumor-bearing mice and breast cancer patients (46). Formaldehyde is considered to be a cancer development risk factor. A recent work showed that in tissues from breast and lung cancer patients, the formaldehyde concentration was 0.75 mmol/L with the highest concentration of 2.35 mmol/L, concentrations being strong enough to activate TRPA1, thereby inducing the secretion of tumor-promoting factors (44). These data suggest that cancer-derived substances (formaldehyde) could have pro-cancer effects by activating TRPA1 in stromal cells, leading to the secretion of the paracrine factors themselves promoting evolution of cancers toward more aggressive forms.

Overall, our data suggest that targeting TRPA1 channel might be an advantage to limit tumor progression. Highlighting the direct effects of Triclosan on the TRPA1 channel expressed in

cancer could allow considering new and/or complementary therapies targeting this channel, and/or preventive measures in the treatment of prostate cancers, which take into account the impact of these environmental factors.

Disclosure of Potential Conflicts of Interest

No potential conflicts of interest were disclosed.

Disclaimer

The funders had no role in study design, data collection and analysis, decision to publish, or preparation of the manuscript.

Authors' Contributions

Conception and design: M. Roudbaraki

Development of methodology: S. Derouiche, M. Roudbaraki, P. Mariot, E. Vancauwenberghe, M. Warnier, G. Bidaux, P. Gosset, E. Dewailly

Acquisition of data (acquired and managed patients, provided facilities, etc.): S. Derouiche, P. Mariot, E. Vancauwenberghe, M. Warnier, P. Gosset, B. Mauroy, J.-L. Bonnal, C. Slomianny

Analysis and interpretation of data (e.g., statistical analysis, biostatistics, computational analysis): M. Roudbaraki, N. Prevarskaya, S. Derouiche, P. Mariot, G. Bidaux, P. Gosset, C. Slomianny,

Writing, review, and/or revision of the manuscript: M. Roudbaraki, S. Derouiche, E. Vancauwenberghe, G. Bidaux, P. Gosset,

Administrative, technical, or material support (i.e., reporting or organizing data, constructing databases): E. Vancauwenberghe, P. Delcourt

Study supervision: M. Roudbaraki

Acknowledgments

We would like to thank Dr. L.R. Sadofsky (Cardiovascular and Respiratory Studies, The University of Hull, Castle Hill Hospital, Cottingham, Hull HU16 5JQ, UK) for the hTRPA1-pCDNA3 expression vector construction and E. Richard for the technical assistance in images analysis by confocal microscopy.

Grant Support

This work was supported by grants from Région Nord Pas-de-Calais (M. Roudbaraki), Institut National de la Santé et de la Recherche Médicale (INSERM; all authors received), the Ministère de l'Éducation Nationale de l'Enseignement Supérieur et de la Recherche (all authors received), and La Ligue Nationale Contre le Cancer (N. Prevarskaya). S. Derouiche was supported by the Région Nord Pas-de-Calais and Association pour la Recherche sur les Tumeurs de la Prostate (ARTP; S. Derouiche and M. Roudbaraki).

The costs of publication of this article were defrayed in part by the payment of page charges. This article must therefore be hereby marked *advertisement* in accordance with 18 U.S.C. Section 1734 solely to indicate this fact.

Received October 11, 2016; revised December 30, 2016; accepted January 3, 2017; published OnlineFirst January 17, 2017.

References

- Denmeade SR, Isaacs JT. A history of prostate cancer treatment. *Nat Rev Cancer* 2002;2:389–96.
- McKenna NJ, O'Malley BW. Minireview: nuclear receptor coactivators—an update. *Endocrinology* 2002;143:2461–5.
- Visakorpi T, Hyytiäinen E, Koivisto P, Tanner M, Keinänen R, Palmberg C, et al. In vivo amplification of the androgen receptor gene and progression of human prostate cancer. *Nat Genet* 1995; 9:401–6.
- Giovannucci E. Nutritional factors in human cancers. *Adv Exp Med Biol* 1999;472:29–42.
- Jankevicius F, Miller SM, Ackermann R. Nutrition and risk of prostate cancer. *Urol Int* 2002;68:69–80.
- Cunha GR, Hayward SW, Wang YZ. Role of stroma in carcinogenesis of the prostate. *Differentiation* 2002;70:473–85.
- Sung SY, Chung LW. Prostate tumor-stroma interaction: molecular mechanisms and opportunities for therapeutic targeting. *Differentiation* 2002;70:506–21.
- Liotta LA, Kohn EC. The microenvironment of the tumour-host interface. *Nature* 2001;411:375–9.
- Wernert N. The multiple roles of tumour stroma. *Virchows Arch* 1997; 430:433–43.
- Wernert N, Locherbach C, Wellmann A, Behrens P, Hugel A. Presence of genetic alterations in microdissected stroma of human colon and breast cancers. *Anticancer Res* 2001;21:2259–64.

11. Bhowmick NA, Moses HL. Tumor-stroma interactions. *Curr Opin Genet Dev* 2005;15:97-101.
12. Bhowmick NA, Neilson EG, Moses HL. Stromal fibroblasts in cancer initiation and progression. *Nature* 2004;432:332-7.
13. Hu M, Polyak K. Microenvironmental regulation of cancer development. *Curr Opin Genet Dev* 2008;18:27-34.
14. West RB, van de Rijn M. Experimental approaches to the study of cancer-stroma interactions: recent findings suggest a pivotal role for stroma in carcinogenesis. *Lab Invest* 2007;87:967-70.
15. Tuxhorn JA, Ayala GE, Rowley DR. Reactive stroma in prostate cancer progression. *J Urol* 2001;166:2472-83.
16. Grossfeld GD, Hayward SW, Tlsty TD, Cunha GR. The role of stroma in prostatic carcinogenesis. *Endocr Relat Cancer* 1998;5:253-70.
17. Wiseman BS, Werb Z. Stromal effects on mammary gland development and breast cancer. *Science* 2002;296:1046-9.
18. Wozniak AL, Bulayeva NN, Watson CS. Xenoestrogens at picomolar to nanomolar concentrations trigger membrane estrogen receptor- α -mediated Ca^{2+} fluxes and prolactin release in GH3/B6 pituitary tumor cells. *Environ Health Perspect* 2005;113:431-9.
19. Pappas TC, Gametchu B, Watson CS. Membrane estrogen receptors identified by multiple antibody labeling and impeded-ligand binding. *FASEB J* 1995;9:404-10.
20. Black JG, Howes D, Rutherford T. Percutaneous absorption and metabolism of Irgasan DP300. *Toxicology* 1975;3:33-47.
21. Tatarazako N, Ishibashi H, Teshima K, Kishi K, Arizono K. Effects of triclosan on various aquatic organisms. *Environ Sci* 2004;11:133-40.
22. Hovander L, Malmberg T, Athanasiadou M, Athanassiadis I, Rahm S, Bergman A, et al. Identification of hydroxylated PCB metabolites and other phenolic halogenated pollutants in human blood plasma. *Arch Environ Contam Toxicol* 2002;42:105-17.
23. Dayan AD. Risk assessment of triclosan [Irgasan] in human breast milk. *Food Chem Toxicol* 2007;45:125-9.
24. Calafat AM, Ye X, Wong LY, Reidy JA, Needham LL. Urinary concentrations of triclosan in the U.S. population: 2003-2004. *Environ Health Perspect* 2008;116:303-7.
25. Ahn KC, Zhao B, Chen J, Cherednichenko G, Sanmarti E, Denison MS, et al. In vitro biologic activities of the antimicrobials triclocarban, its analogs, and triclosan in bioassay screens: receptor-based bioassay screens. *Environ Health Perspect* 2008;116:1203-10.
26. Kumar V, Chakraborty A, Kural MR, Roy P. Alteration of testicular steroidogenesis and histopathology of reproductive system in male rats treated with triclosan. *Reprod Toxicol* 2009;27:177-85.
27. Gee RH, Charles A, Taylor N, Darbre PD. Oestrogenic and androgenic activity of triclosan in breast cancer cells. *J Appl Toxicol* 2008;28:78-91.
28. Chen J, Ahn KC, Gee NA, Gee SJ, Hammock BD, Lasley BL. Antiandrogenic properties of parabens and other phenolic containing small molecules in personal care products. *Toxicol Appl Pharmacol* 2007;221:278-84.
29. Kumar V, Balomajumder C, Roy P. Disruption of LH-induced testosterone biosynthesis in testicular Leydig cells by triclosan: probable mechanism of action. *Toxicology* 2008;250:124-31.
30. Wong CK, Lai T, Holly JM, Wheeler MH, Stewart CE, Farndon JR. Insulin-like growth factors (IGF) I and II utilize different calcium signaling pathways in a primary human parathyroid cell culture model. *World J Surg* 2006;30:333-45.
31. Gackiere F, Bidaux G, Lory P, Prevarskaya N, Mariot P. A role for voltage gated T-type calcium channels in mediating "capacitative" calcium entry? *Cell Calcium* 2006;39:357-66.
32. Lallet-Daher H, Roudbaraki M, Bavencoffe A, Mariot P, Gackiere F, Bidaux G, et al. Intermediate-conductance Ca^{2+} -activated K^{+} channels (IKCa1) regulate human prostate cancer cell proliferation through a close control of calcium entry. *Oncogene* 2009;28:1792-806.
33. Fajardo O, Meseguer V, Belmonte C, Viana F. TRPA1 channels: novel targets of 1,4-dihydropyridines. *Channels (Austin)* 2008;2:429-38.
34. Gu Q, Lin RL. Heavy metals zinc, cadmium, and copper stimulate pulmonary sensory neurons via direct activation of TRPA1. *J Appl Physiol* 2010;108:891-7.
35. Hinman A, Chuang HH, Bautista DM, Julius D. TRP channel activation by reversible covalent modification. *Proc Natl Acad Sci U S A* 2006;103:19564-8.
36. Hu H, Tian J, Zhu Y, Wang C, Xiao R, Herz JM, et al. Activation of TRPA1 channels by fenamate nonsteroidal anti-inflammatory drugs. *Pflugers Arch* 2010;459:579-92.
37. Meseguer V, Karashima Y, Talavera K, D'Hoedt D, Donovan-Rodriguez T, Viana F, et al. Transient receptor potential channels in sensory neurons are targets of the antimycotic agent clotrimazole. *J Neurosci* 2008;28:576-86.
38. Andrade EL, Meotti FC, Calixto JB. TRPA1 antagonists as potential analgesic drugs. *Pharmacol Ther* 2012;133:189-204.
39. Cao DS, Zhong L, Hsieh TH, Abooj M, Bishnoi M, Hughes L, et al. Expression of transient receptor potential ankyrin 1 (TRPA1) and its role in insulin release from rat pancreatic beta cells. *PLoS One* 2012;7:e38005.
40. Story GM, Peier AM, Reeve AJ, Eid SR, Mosbacher J, Hricik TR, et al. ANKTM1, a TRP-like channel expressed in nociceptive neurons, is activated by cold temperatures. *Cell* 2003;112:819-29.
41. Wong YC, Wang YZ. Growth factors and epithelial-stromal interactions in prostate cancer development. *Int Rev Cytol* 2000;199:65-116.
42. Skobe M, Hawighorst T, Jackson DG, Prevo R, Janes L, Velasco P, et al. Induction of tumor lymphangiogenesis by VEGF-C promotes breast cancer metastasis. *Nat Med* 2001;7:192-8.
43. Andersson DA, Gentry C, Moss S, Bevan S. Transient receptor potential A1 is a sensory receptor for multiple products of oxidative stress. *J Neurosci* 2008;28:2485-94.
44. Tong Z, Luo W, Wang Y, Yang F, Han Y, Li H, et al. Tumor tissue-derived formaldehyde and acidic microenvironment synergistically induce bone cancer pain. *PLoS One* 2010;5:e10234.
45. Spanel P, Smith D, Holland TA, Al Singary W, Elder JB. Analysis of formaldehyde in the headspace of urine from bladder and prostate cancer patients using selected ion flow tube mass spectrometry. *Rapid Commun Mass Spectrom* 1999;13:1354-9.
46. Ebeler SE, Clifford AJ, Shibamoto T. Quantitative analysis by gas chromatography of volatile carbonyl compounds in expired air from mice and human. *J Chromatogr B Biomed Sci Appl* 1997;702:211-5.

Cancer Prevention Research

Activation of TRPA1 Channel by Antibacterial Agent Triclosan Induces VEGF Secretion in Human Prostate Cancer Stromal Cells

Sandra Derouiche, Pascal Mariot, Marine Warnier, et al.

Cancer Prev Res 2017;10:177-187. Published OnlineFirst January 17, 2017.

Updated version	Access the most recent version of this article at: doi:10.1158/1940-6207.CAPR-16-0257
Supplementary Material	Access the most recent supplemental material at: http://cancerpreventionresearch.aacrjournals.org/content/suppl/2017/01/16/1940-6207.CAPR-16-0257.DC1

Cited articles	This article cites 46 articles, 5 of which you can access for free at: http://cancerpreventionresearch.aacrjournals.org/content/10/3/177.full#ref-list-1
-----------------------	---

E-mail alerts	Sign up to receive free email-alerts related to this article or journal.
Reprints and Subscriptions	To order reprints of this article or to subscribe to the journal, contact the AACR Publications Department at pubs@aacr.org .
Permissions	To request permission to re-use all or part of this article, use this link http://cancerpreventionresearch.aacrjournals.org/content/10/3/177 . Click on "Request Permissions" which will take you to the Copyright Clearance Center's (CCC) Rightslink site.